Immunity, Volume *54*

Supplemental information

A potently neutralizing SARS-CoV-2 antibody inhibits variants of concern by utilizing unique binding residues in a highly conserved epitope

Laura A. VanBlargan, Lucas J. Adams, Zhuoming Liu, Rita E. Chen, Pavlo Gilchuk, Saravanan Raju, Brittany K. Smith, Haiyan Zhao, James Brett Case, Emma S. Winkler, Bradley M. Whitener, Lindsay Droit, Ishmael D. Aziati, Traci L. Bricker, Astha Joshi, Pei-Yong Shi, Adrian Creanga, Amarendra Pegu, Scott A. Handley, David Wang, Adrianus C.M. Boon, James E. Crowe Jr., Sean P.J. Whelan, Daved H. Fremont, and Michael S. Diamond

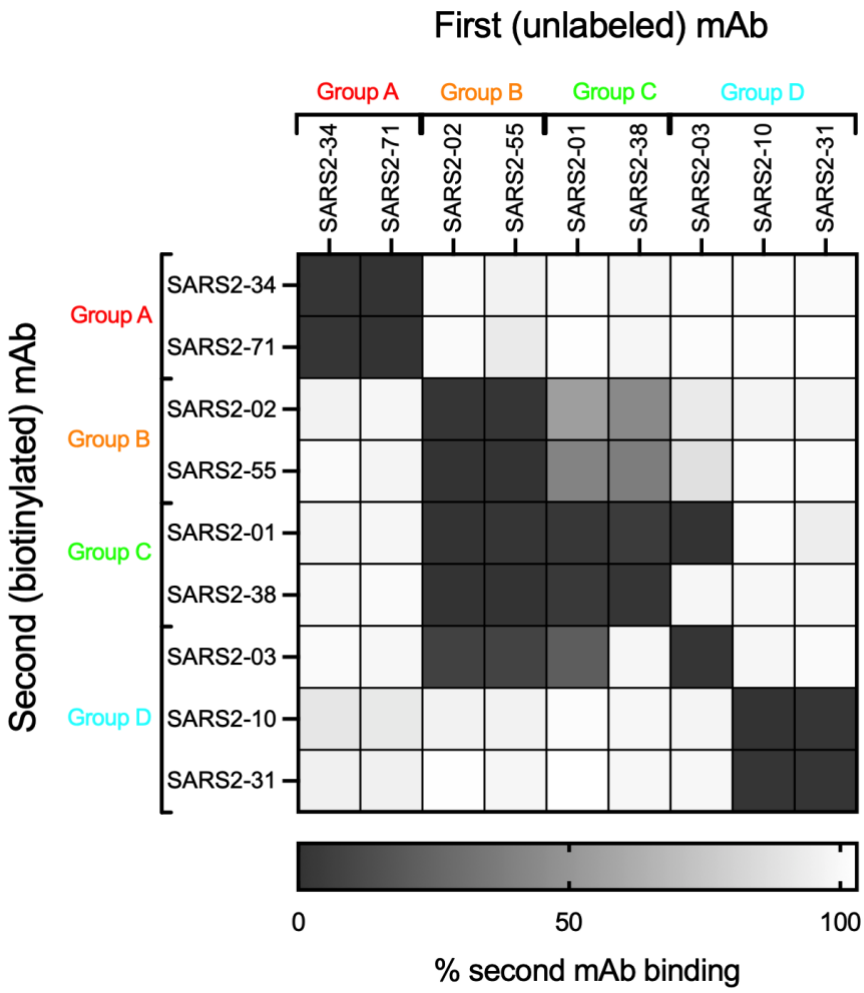

Figure S1. Competition profile of mAb panel, Related to Figure 1. A subset of mAbs from each reference mAb competition group were tested for competition for SARS-CoV-2 spike binding against each other. Data represent mean of technical duplicates.

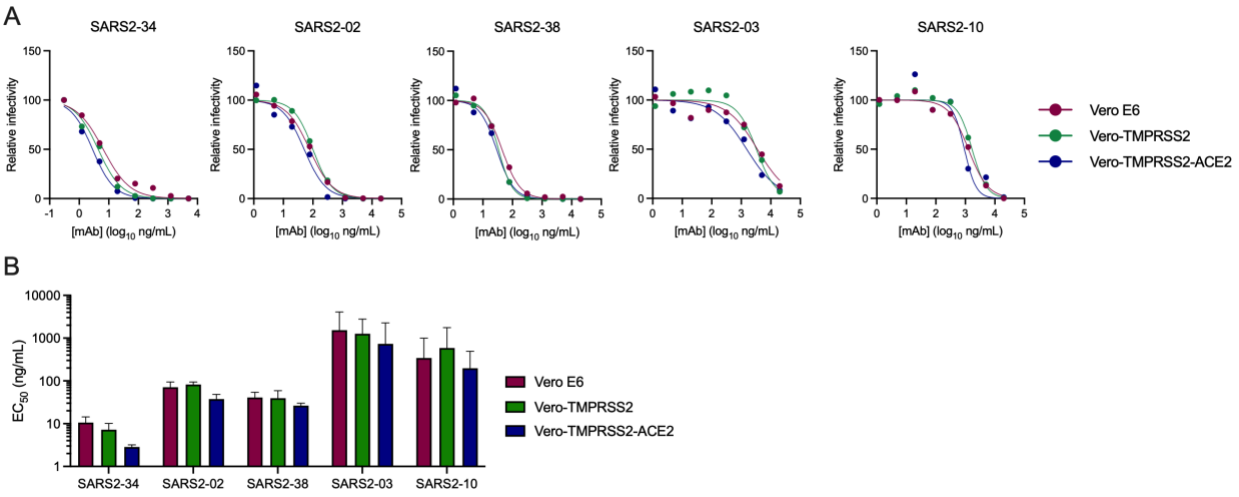

Figure S2. Neutralization by anti-SARS-CoV-2 mAbs on different cell substrates, Related to Figure 2. Anti-SARS-CoV-2 mAbs were assayed for neutralization by FRNT against SARS-CoV-2 using Vero E6, Vero-TMPRSS2, Vero-TMPRSS2-ACE2. (**A**) Representative dose response curves are shown. (**B**) Mean EC50 values are shown; Error bars represent SEM from three experiments.

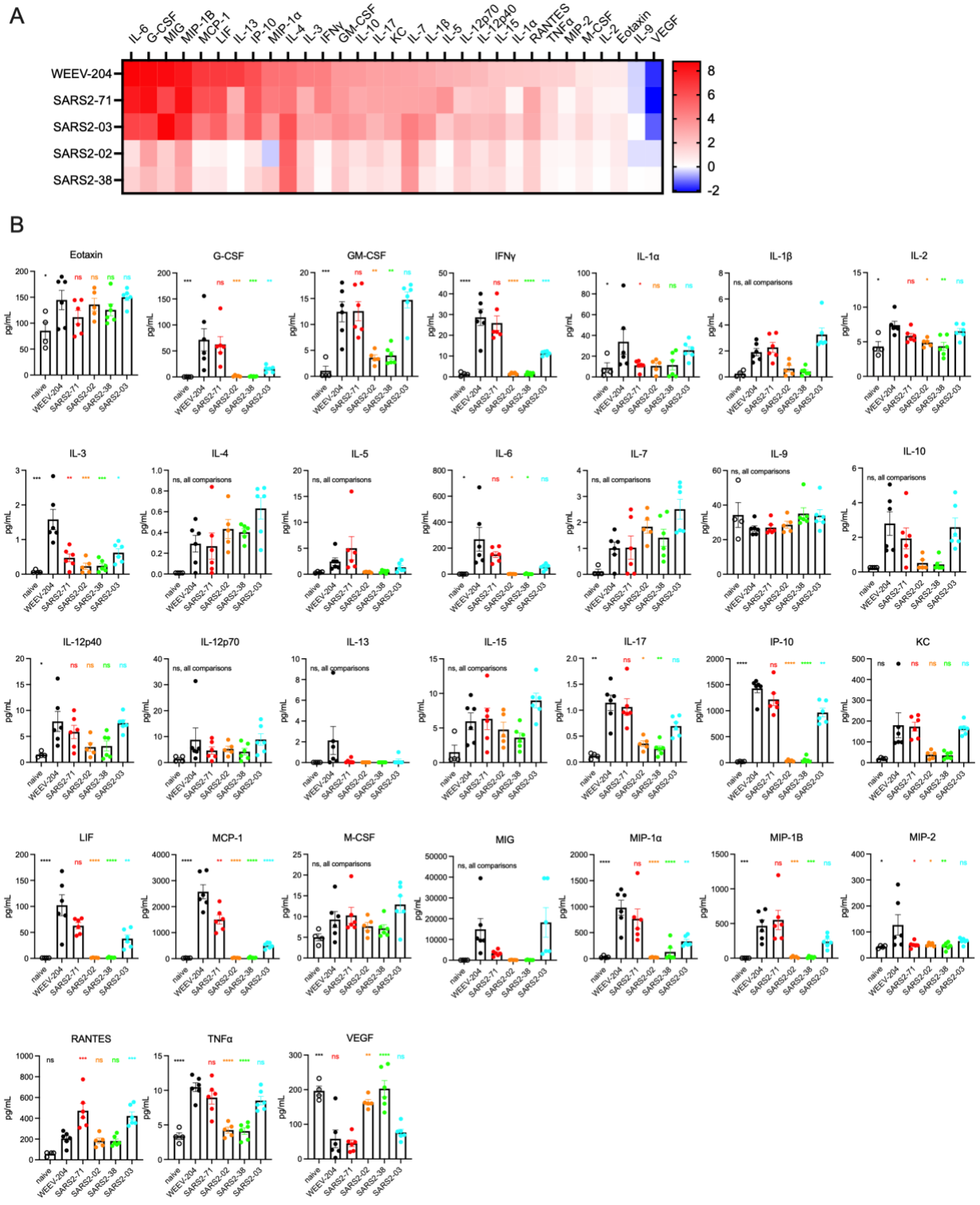

Figure S3. Cytokine and chemokine levels in the lungs of SARS-CoV-2 infected mice following treatment with anti-SARS-CoV2 mAbs, Related to Figure 4. Cytokine and chemokine levels in lung homogenates harvested in **Fig 4** were measured by a multiplex platform. (**A**) Heat map showing Log_2 fold change in cytokine and chemokine levels compared to lungs from mock-infected animals. (**B**) Levels of each cytokine and chemokine are plotted. Data are from two experiments, n = 5-6 per group. Error bars represent SEM. One-way ANOVA with Dunnett's post-test: ns, not significant, *p < 0.05, **p < 0.01, ***p < 0.001, ****p < 0.0001.)

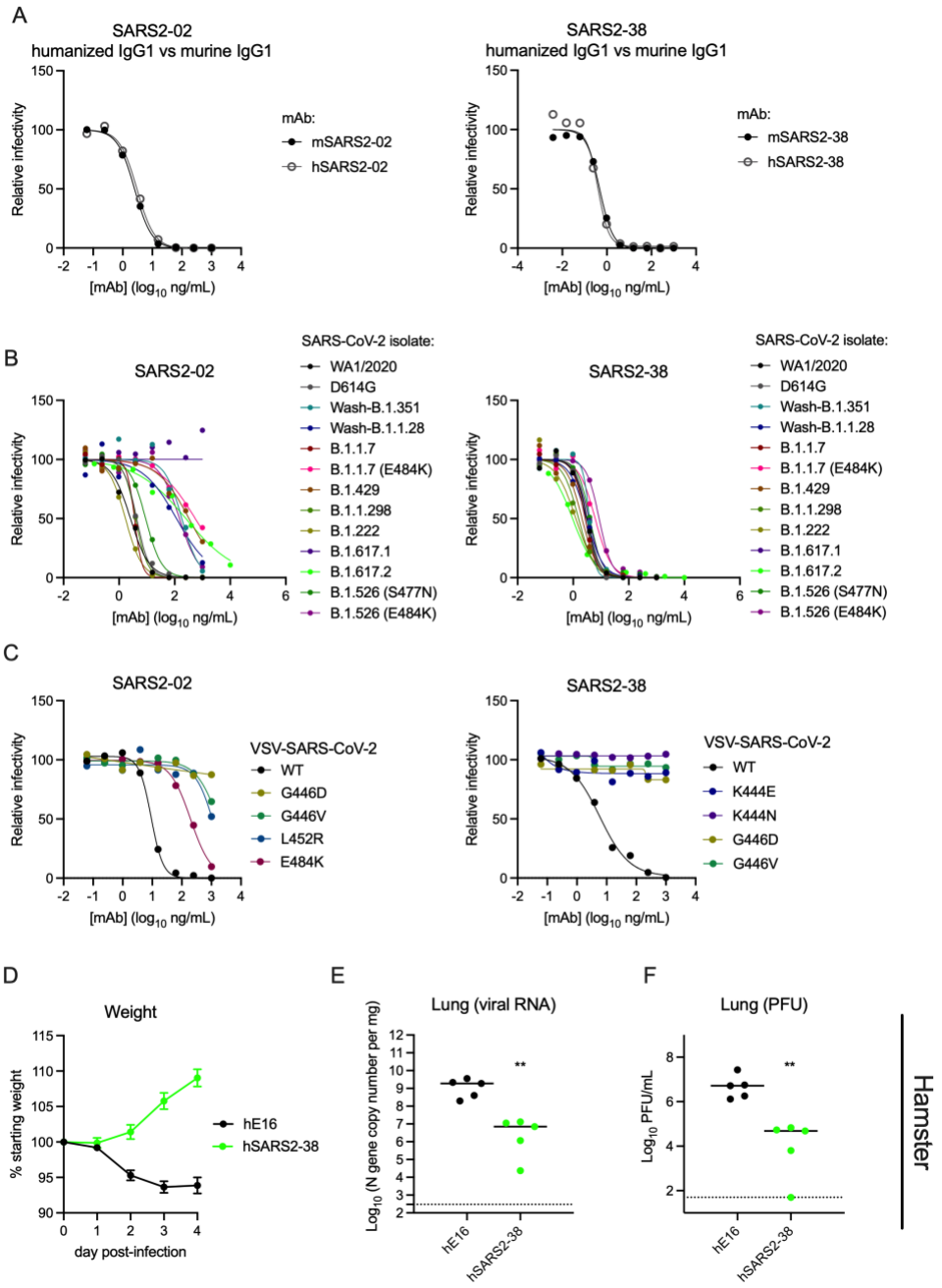

Figure S4. **Neutralization of SARS-CoV-2 variants and *in vivo* protection by SARS2-38 and SARS2-02, Related to Figures 4 and 5. (A)** Anti-SARS-CoV-2 chimeric mouse Fv/human IgG1 Fc mAbs were assayed for neutralization by FRNT against SARS-CoV-2 WA/2020. m, mouse hybridoma-derived mAb, and h, recombinant chimeric mAb. Representative dose response curves are shown. Data are from three experiments. (**B**) Representative dose response curves of neutralization of SARS-CoV-2 variants by SARS2-02 and SARS2-38. Mean EC50 values from all independent experiments are shown in **Fig 5**. (**C**) Representative dose response curves of SARS2-02 and SARS2-38 neutralization of VSV-eGFP-SARS-CoV-2-S and the indicated neutralization-resistant mutants. Data is from of one of two experiments. (**D-F**) Syrian golden hamsters were administered 1 mg (~10 mg/kg) of the indicated mAb and 24 h later they were infected with $5x10^5$ PFU of SARS-CoV-2 Wash-B.1.351. (**D**) Mean weight change. Error bars represent SEM. (**E-F**) At 4 dpi, lungs were collected and the level of viral RNA (**E**) and infectious virus (**F**) was determined (Mann Whitney test, **p < 0.01,). Median value is shown. Data are from one experiment; n = 5 for all groups.

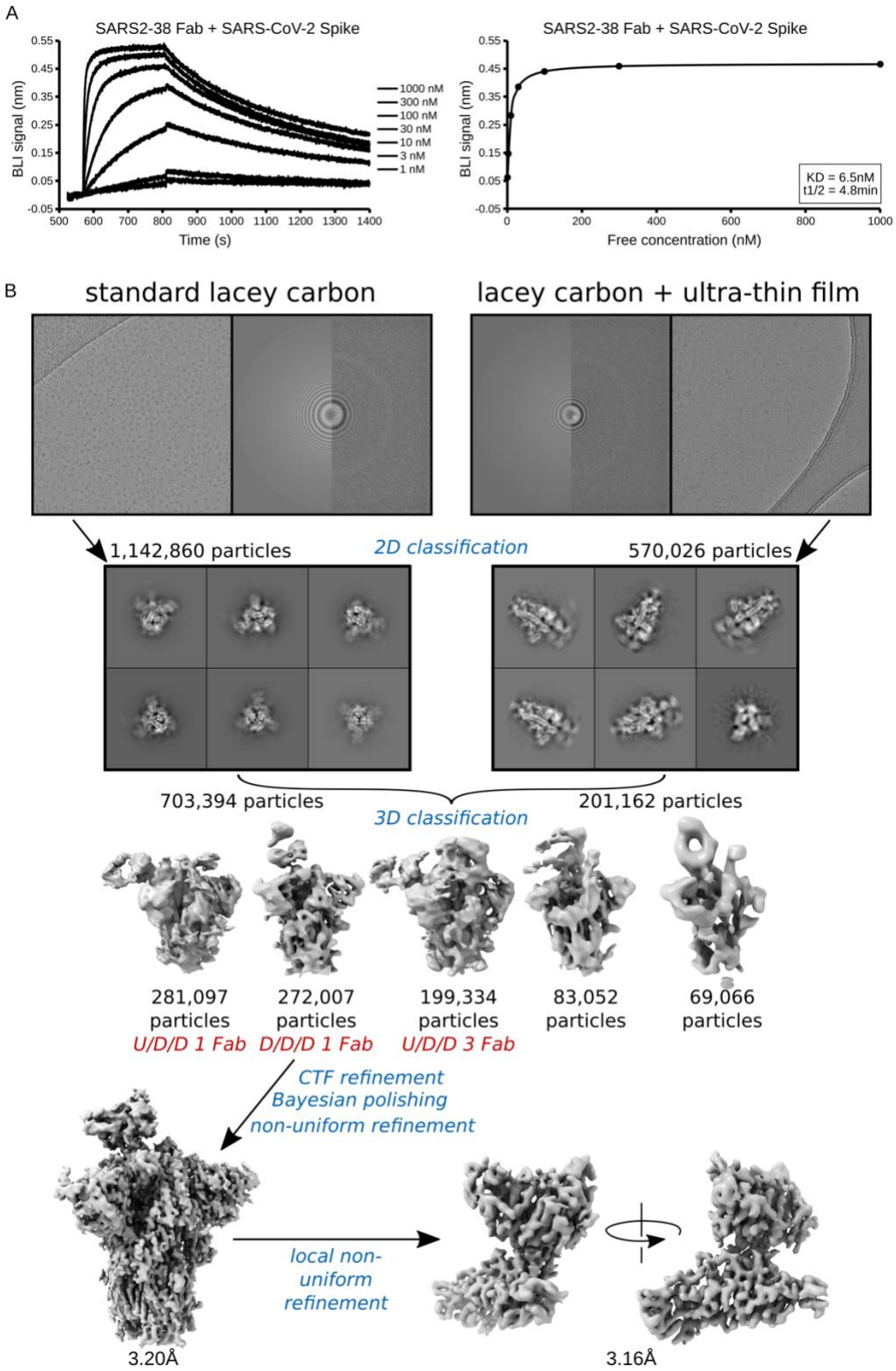

Figure S5. Binding analysis and cryo-EM data processing pipeline, Related to Figure 6. (**A**) Biolayer interferometry signal (left) and steady state analysis (right) of SARS2-38 Fab interacting with immobilized SARS-CoV-2 spike. Kinetic values were fitted to a 1:1 binding model with a drifting baseline. (**B**) Flowchart depicting data processing steps for global reconstruction of SARS2-38 Fv bound to trimeric spike and local refinement of SARS2-38 Fv bound to RBD.

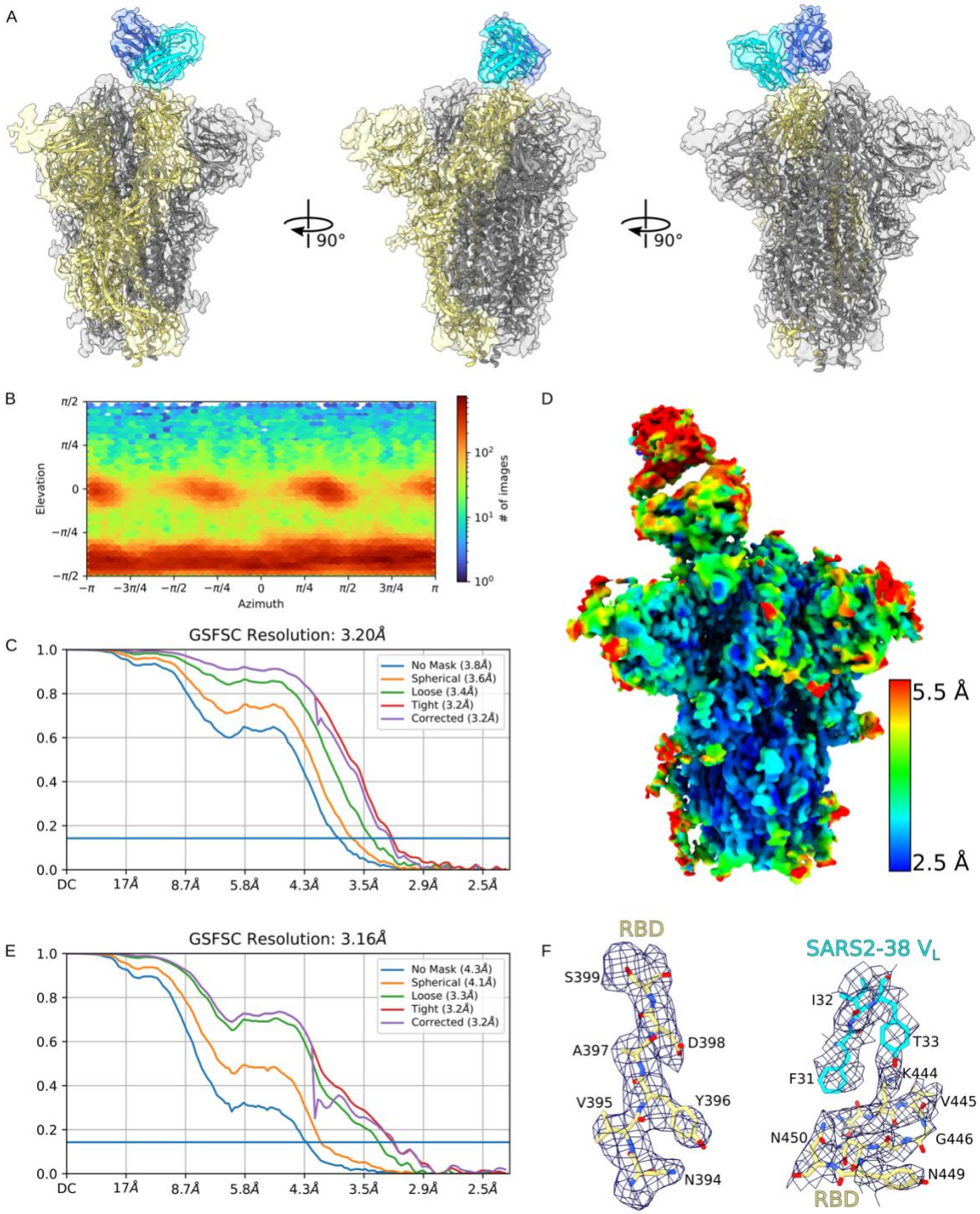

Figure S6. Validation of global and local cryo-EM reconstructions of SARS2-38 Fv bound to SARS-CoV-2 spike/RBD, Related to Figure 6. (**A**) Density map and fitted model of SARS2-38 Fv bound to trimeric SARS-CoV-2 spike. The spike monomer bound by SARS2-38 is shown in yellow, with the rest of the trimer colored gray. The SARS2-38 heavy chain is shown in royal blue, and the light chain in cyan. (**B**) Orientational distribution assigned to particles in global refinement of SARS2-38 Fv bound to trimeric spike. (**C**) GSFSC curve for global refinement of SARS2-Fv bound to trimeric spike. (**D**) Local resolution map for global refinement of SARS2-38 Fv bound to trimeric spike. (**E**) GSFSC curve for local refinement of SARS2-Fv bound to RBD. (**F**) Example density and model fits for an RBD beta strand (left) and at the SARS2-38/RBD interface (right). RBD, yellow; SARS2-38 light chain, cyan.

Table S1. Cryo-EM data collection, processing, and model refinement statistics, Related to Figure 6.

	SARS-CoV-2 spike + Fv SARS2-38 (full) PDB 7MKL EMD-23898	SARS-CoV-2 RBD + Fv SARS2-38 (local) PDB 7MKM EMD-23899
Data collection		
Magnification	59,000x	59,000x
Exposure ($e^-/Å^2$)	50	50
Defocus range (μm)	0.8-2.3	0.8-2.3
Pixel size (Å/pixel)	1.16	1.16
Data processing		
Initial particles (no.)	1,712,886	1,712,886
Final particles (no.)	272,007	272,007
Nominal resolution (Å)	3.20	3.16
FSC threshold	0.143	0.143
Model refinement		
Adapted PDB models	6M0J, 1KIQ, 5XJM, 6VXX	6M0J, 1KIQ, 5XJM
Model resolution (Å)	4.1	4.2
FSC threshold	0.5	0.5
Model composition		
Non-hydrogen atoms	25,597	3,192
Residues	3,164	406
Ligands	63	1
B-factors ($Å^2$)		
Residues	96.29	54.21
Ligands (glycans)	116.22	76.57
Bonds (RMSD)		
Length (Å)	0.004	0.0032
Angles (°)	0.782	0.806
Validation		
Molprobity score	1.66	1.55
Clash score	9.83	7.53
Rotamer outliers (%)	0.00	0.00
Ramachandran		
Favored (%)	97.19	97.25
Allowed (%)	2.81	2.75
Outliers (%)	0.0	0.0

Respective statistics are provided for local and global refinements of SARS2-38 Fv bound to SARS-CoV-2 RBD/spike.

Table S2. Close contacts and buried surface area of SARS2-38/RBD interface, Related to Figure 6.

RBD epitope residue	SARS2-38 residue (no. close contacts)	Buried surface area, Å^2 (% of interface)
T345	-	3.9 (0.7%)
N439	-	7.3 (1.4%)
N440	N91^L(6)	65.1 (12.3%)
L441	S30^L(3), F31^L(2), N91^L(3)	64.1 (12.1%)
D442	F31^L(2)	7.9 (1.5%)
S443	F31^L(1), N91^L(1)	20.6 (3.9%)
K444	F31^L(1), Y33^L(3), W90^L(3)	85.8 (16.2%)
V445	W90^L(4), Y93^L(1)	102.3 (19.3%)
G446	-	21.0 (4.0%)
N448		2.6 (0.5%)
Y449	R100^H(7)	50.1 (9.4%)
N450	R100^H(1)	29.3 (5.5%)
Y451		4.3 (0.8%)
P499	-	39.3 (7.4%)
T500	Y58^H(1)	27.1 (5.1%)

RBD epitope residues were determined via PISA solvent exclusion analysis. Close contact residues of mAb SARS2-38 are listed for each RBD residue, with the number of pairwise atomic contacts noted for each interaction (< 3.9 Å cutoff). SARS2-38 residues are superscripted to delineate light chain (L) and heavy chain (H) residues. Buried surface area was calculated using the Shrake-Rupley algorithm as implemented in the MDTraj python library.

Table S3. Summary of mAbs that bind similar or proximal epitopes to SARS2-38 and associated structural and functional data, Related to Figures 6 and 7.

mAb	Structural binding site	Functional Residues	in vivo studies (prophylaxis & therapeutic)	Neutralization potency (authentic virus [AV] or pseudovirus [PV])	Mechanism of action	Variant neutralization (authentic virus [AV] or pseudovirus [PV])	References (Published)	References (Preprint)
SARS2-38	345, 439-446, 448-451, 499-500	VSV-SARS-CoV-2 escape: K444E/N, G446D/V	Prophylactic and therapeutic protection in K18-ACE2 transgenic mice following infection with WA1/2020, B.1.351 (Wash-B.1.351 Spike chimeric virus), and B.1.617.1	5 ng/mL (AV), 6 ng/mL (PV-VSV)	ACE2 blocking	Neutralizes (AV): B.1.1.7, B.1.429, B.1.1.28, B.1.351, B.1.222, B.1.1.298, B.1.617.1, B.1.617.2, B.1.526+S477N, B.1.526+E484K, B.1.1.7+E484K	This paper	
2H04	337, 339-340, 343-346, 356, 439-445, 448, 450, 499, 509	VSV-SARS-CoV-2 escape: T345A/N/S, R346G, L441R, K444R,	Prophylactic protection in K18-ACE2 transgenic mice following infection with WA1/2020	279 ng/mL (AV)	Non-ACE2 blocking		Alsoussi et al., 2020; Liu et al., 2021	
REGN 10987	346, 439-441, 443-450, 498-501	Mutational analysis/yeast display: N439, N440, K444, V445, G446, G447, N448, N439, N440, P499	Cocktail of REGN1098+REGN10933 protects against N501Y/D614G, B.1.1.7, B.1.351, and B.1.1.28 in K18-ACE2 transgenic mice (prophylaxis and post-exposure therapy) and in 129S mice (prophylaxis)	12ng/mL/4.21E-11 M (AV); 4.06E-11 (PV-VSV)	ACE2 blocking	Neutralizes (AV): B.1.1.7, B.1.351, B.1.1.28; Decreased potency against (AV) B.1.429, B.1.617.1, B.1.526, and (PV) N349K	Chen et al., 2021c; Hansen et al., 2020; Thomson et al., 2021	
S309	333-335, 337, 339-341, 343-346, 354, 356-361, 440-441, 444. 509	Mutational analysis/yeast display: P337, E340 VSV-SARS-CoV-2 escape: E340A/K/G, P337L Authentic SARS-CoV-2 escape: E340A	Cocktail of S309+S2E12 protects against N501Y/D614G, B.1.1.7, B.1.351, and B.1.1.28 in K18-ACE2 transgenic mice (prophylaxis and post-exposure therapy) and in 129S mice (prophylaxis)	79 ng/mL (AV)	Non-ACE2 blocking	Neutralizes (AV): B.1.351, B.1.1.28, B.1.429, B.1.617.1, B.1.526, and (PV) N439K; Reduced neutralization of B.1.1.7 (variably), E484K+N501Y+D614G and (PV-MLV) SARS-CoV	Chen et al., 2021c; Chen et al., 2021d; Pinto et al., 2020; Starr et al., 2021; Wang et al., 2021	
COV2-2130	345-346, 439-441, 443-447, 449-450, 452, 484, 490. 492-494, 499	Mutational analysis/yeast display: R346, K444, G447, N448 VSV-SARS-CoV-2 escape: K444R/E Authentic SARS-CoV-2 escape: N74K, R346I	Cocktail of COV2-2130+COV2-2196 protects against N501Y/D614G, B.1.1.7, B.1.351, and B.1.1.28 in K18-ACE2 transgenic mice (prophylaxis and post-exposure therapy) and in 129S mice (prophylaxis) and against B.1.351 in hamsters (prophylaxis)	26 ng/mL (AV)	ACE2 blocking	Neutralizes (AV): B.1.1.7, B.1.351, B.1.1.28, and B.1.526; slightly decreased potency against B.1.429, B.1.617.1, and E484K/D614G	Chen et al., 2021c	Dong et al., 2021
C110	344-347, 351, 441-442, 448-452, 470, 490, 492, 494, 498-500, 509		Prophylactic protection against mouse-adapted SARS-COV-2 in BALB/c mice	18 ng/mL (PV - HIV)	May sterically interfere with ACE2 binding		Barnes et al., 2020; Robbiani et al., 2020; Schäfer et al., 2021	

C119	403, 405, 444-450, 452-453, 484, 490, 492-495, 497-505			9 ng/mL (PV - HIV)	ACE2 blocking		Barnes et al., 2020; Robbiani et al., 2020; Schäfer et al., 2021	
COVOX-75	417, 421, 453, 455-458, 473-480, 484-489, 493						Dejnirattisai et al., 2021	
2-7	345-346, 439-450, 498-503, 506			3 ng/mL (AV), 10 ng/mL (PV-VSV)	ACE2 blocking	Neutralizes (PV): B.1.1.7, B.1.351	Cerutti et al., 2021; Liu et al., 2020; Wang et al., 2021	
BG10-19	335, 338, 339, 342-346, 367, 368, 371, 373, 374, 437-439, 440-446, 478, 450-451, 499, 500, 509, and NTD glycan at N165 (Quaternary epitope bridging 2 RBDs and NTD)	VSV-SARS-CoV-2 escape: L441P, G339R		33 ng/mL (AV), 9 ng/mL (PV-HIV)	inhibits exposure of the ACE2 RBM, by locking the S trimer into a closed conformation	Neutralizes (PV): B.1.1.7, B.1.351, SARS-CoV, PVs with single amino acid changes from VOCs (R683G, N439K, Y453F, N501Y, R346S)	Scheid et al., 2021	
BG7-15	439–44, 443-450, 452, 490, 492-494, 499, 500, 506	Mutational analysis (binding RBD mutants by ELISA): V445E, Q498Y/P499T PV neutralization: K444Q, V445E, N439K (slight decrease)		114 ng/mL (AV), 16 ng/mL (PV-HIV)	Sterically hinders ACE2 binding	Neutralizes (PV): B.1.1.7, B.1.351, PV with single amino acid change N439K (with some decrease in potency)	Scheid et al., 2021	
DH1047	368-372, 374-381, 383, 384, 404, 405, 407-409, 414-416, 435, 499, 501-506, 508		SARS-CoV-2 (Cynomolgus macaques, 10mg/kg, prophylaxis); SARS-CoV-2 B.1.351 (aged mouse model, prophylactic protection, therapeutic administration reduced viral titers in lung and lung pathology but not weight loss) and cross-protection against WIV1-CoV (in HFH4-ACE2-transgenic mice, administered 12 h pre or post-infection; 300ug Ab); SARS-CoV (MA15 model, prophylaxis and 12 h post-infection, 10mg/kg); RsSHC014	398 ng/mL (AV), 90 ng/mL (PV-lentivirus)	ACE2 blocking	Neutralizes (AV and PV):B.1.1.7, B.1.429, B.1.351, SARS-CoV, WIV-1, RsSHC014	Li et al., 2021a	Martinez et al., 2021
S2H97	353, 355, 357, 393, 394, 396, 426-430, 459, 460,	Mutational analysis (yeast display): N394, Y396, D428, K462,		749 ng/mL (AV), 338 ng/mL (PV-VSV)		Neutralizes (PV): SARS-CoV GD-Pangolin, RTG13, GX-Pangolin, WIV-1		Starr et al., 2021

	462-466, 514-516, 518	S514, E516, L518						
S2×259	369-386, 404, 407, 408, 471, 474, 479-481	Mutational analysis (yeast display): G504 VSV-SARS-CoV-2 escape: G504D	Prophylactic protection in Syrian hamster model (Wuhan-1 strain, 4mg/kg mAb)	144 ng/mL (AV), 87 ng/mL (PV-MLV), 213 ng/mL (VSV PV-VSV)	ACE2 blocking	Neutralizes (PV): B.1.1.7, B.1.351, P.1, B.1.427/B.1.429, N439K, Y453F, Pangolin GD, RaTG13, SARS-CoV, WIV1, WIV16, SHC014	Thomson et al., 2021	Tortorici et al., 2021